



Iranian Association of  
Electrical and Electronics  
Engineers

# Journal of Applied Research in Electrical Engineering

E-ISSN: 2783-2864

P-ISSN: 2717-414X

Homepage: <https://jaree.scu.ac.ir/>



## Research Article

### Voltage and Frequency Control Considering Disturbance in Input Power of DG

Ali Morsagh Dezfuli<sup>1</sup> , Mahyar Abasi<sup>2,3,\*</sup> , Mohammad Esmaeil Hasanzadeh<sup>4</sup> , and Mahmood Joorabian<sup>1</sup> 

<sup>1</sup> Department of Electrical Engineering, Faculty of Engineering, Shahid Chamran University of Ahvaz, Ahvaz 61357-85311, Iran

<sup>2</sup> Department of Electrical Engineering, Faculty of Engineering, Arak University, Arak 38156-8-8349, Iran

<sup>3</sup> Research Institute of Renewable Energy, Arak University, Arak 38156-8-8349, Iran

<sup>4</sup> Department of Electrical Engineering, Firouzabad Higher Education Center, Shiraz University of Technology, Shiraz, Iran

\* Corresponding Author: [m-abasi@araku.ac.ir](mailto:m-abasi@araku.ac.ir)

**Abstract:** The utilization of distributed generation (DG) in today's power systems has led to the emergence of the concept of microgrids, in addition to changing the mode of generating and supplying the energy required for network electrical loads. When a microgrid operates in the island mode, energy generation sources are responsible for controlling the microgrid's voltage and frequency. As the microgrid frequency is proportional to the amount of power generated by the DG, the microgrid requires a precise power-sharing strategy. Considering that DGs do not usually have stable output power despite the importance of power stability, the present paper addresses the voltage and frequency control of an islanded microgrid by considering the power generation uncertainties caused by disturbances and the varying power output of DGs. Given that the disturbance on the first DG's input current is 0.2 A, which is approximately 2.2% of the steady-state value, a simulation was performed, and it was observed that the maximum voltage variation of each bus in the worst case was 0.59% for the first bus and 0.53% for the second bus, which means that the controller could control the voltage and frequency values within the permissible range. If the controller is not used, the change in the frequency of each bus will be 10 times, and the voltage change will be 5 times as great as that of the case the controller is used.

**Keywords:** Microgrid, frequency control, voltage control, distributed generation.

#### Article history

Received 20 November 2023; Revised 20 January 2024; Accepted 12 February 2024; Published online 19 May 2024.

© 2024 Published by Shahid Chamran University of Ahvaz & Iranian Association of Electrical and Electronics Engineers (IAEEE)

#### How to cite this article

Ali Morsagh Dezfuli, Mahyar Abasi, Mohammad Esmaeil Hasanzadeh, and Mahmood Joorabian, "Voltage and frequency control considering disturbance in input power of DG," *J. Appl. Res. Electr. Eng.*, vol. 3, no. 1, pp. 9-18, 2024.

DOI: [10.22055/jaree.2024.45325.1088](https://doi.org/10.22055/jaree.2024.45325.1088)



## 1. INTRODUCTION

The incorporation of DGs in today's power systems has changed the mode of electrical energy generation and supply for electrical loads inside microgrids. This form of the use of DGs does not suffer from energy losses occurring in energy transmission lines, and it covers the discussion of reserve services and the provision of the demanded reactive power. Connecting these resources to the grid requires the adoption of power electronic converters. An electronic power converter can respond to fast load changes and provide fast and flexible control of voltage and frequency, so active and reactive power can be properly controlled. However, the use of DG units complicates the structure and brings about challenges in the operation, control, stability, protection, and security of power distribution networks [1]. Therefore, there are new strategies for connecting these resources to the power system. Islanded microgrids are inherently weak in frequency

and voltage stabilization. Frequency and voltage are highly variable concerning active and reactive power variations, respectively.

Ref. [2] proposed an optimization-based scheme for simultaneous frequency and voltage control in islanded microgrids in which the DG unit with the largest capacity served as the master controller, ensuring proper load sharing. In [3], a finite-time event-triggered control was proposed for frequency and voltage in islanded AC microgrids, enabling efficient power sharing among distributed generators. A two-stage economic plan was suggested in [4] for integrating synchronous distributed generations (SDGs) into distribution networks. The results on standard distribution networks confirmed improved protection coordination and economic indices compared to power flow studies. The authors in [5] attempted a control strategy for microgrid PV inverters, ensuring seamless transitions between grid-connected and

islanding modes. The approach enhanced overall microgrid reliability by mitigating transient variations in voltage, current, phase, frequency, and DC-link voltage. Ref. [6] focused on a washout filter-based power-sharing approach in microgrids, eliminating voltage and frequency deviations without secondary control or communication links. Ref. [7] introduced a multi-agent-based adaptive controller for microgrids, addressing uncertainties in distributed generating resources. Compared to a secondary voltage controller, it demonstrated faster convergence and improved performance in handling load changes. Researchers in [8] presented an event-triggered distributed control for islanded AC microgrids, allowing asynchronous communication without synchronization, effectively reducing communication rates. A fully distributed optimal control for AC microgrids was introduced in [9], emphasizing transient responses. The proposed two-loop control optimized local frequency and voltage adjustments, effectively solving the distributed optimization problem with ADMM and the Lyapunov function approach. Ref. [10] focused on a novel distributed control scheme for islanded microgrids, ensuring finite-time restoration of generator frequencies, active power sharing, and voltage regulation. Ref. [11] investigated efficient islanded microgrid frequency control by coordinating reactive power between a solid oxide fuel cell (SOFC) and a battery, reducing the need for energy storage and eliminating reserve capacity. Ref. [12] introduced a multi-agent adaptive controller for microgrids, comparing its performance with a secondary voltage controller. Ref. [13] explored improving microgrid control during grid-independent operation. It presented a novel optimization approach in which teaching-learning-based optimization and harmonic search algorithms were combined to enhance voltage and frequency regulation. Researchers in [14] introduced a novel evolutionary algorithm for unit commitment, addressing societal quality of life improvement with thermal and wind units. Ref. [15] proposed disturbance observer-based control for regulating frequency and voltage in a low-inertia microgrid with solar PV and a diesel generator. A distributed control approach was proposed in [16] for islanded microgrids, optimizing reactive power-sharing and addressing voltage/frequency drop issues. A decoupled double synchronous reference frame-based virtual synchronous generator (VSG) was introduced in [17] for improved performance in unbalanced conditions within an islanded microgrid. The method enhanced controllability, accuracy, and robustness under heavy loads by separating positive and negative components. Ref. [18] optimally allocated DG units in networks with unbalanced loads using a modified group search optimizer (GSO) algorithm. Ref. [19] investigated an efficient power control technique for inverter-based DG in an islanded microgrid and emphasized improved electricity quality during islanded operation. The control method integrated internal current and external power control loops. An adaptive virtual impedance control method optimized by the multi-objective particle swarm optimization (MOPSO) algorithm was considered for efficient voltage and frequency control in microgrids [20]. Ref. [21] introduced a fixed-time control approach for islanded AC microgrids that utilized a multi-agent consensus method with an adaptive fuzzy fixed-time secondary voltage controller and a secondary frequency controller based on the control barrier function. A disturbance-observer-based control (DOBC) was proposed in [22] for efficient frequency and voltage

regulation in power systems with high renewable energy sources (RES). Ref. [23] introduced two event-triggered fault-tolerant control (ETFTC) algorithms for voltage restoration in microgrids, addressing bias faults in distributed generators' actuators and reliability in distributed control applications. Researchers in [24] discussed an advanced power-sharing control method using sliding mode control in microgrids. It improved voltage quality and enhanced power-sharing accuracy among inverters, even during communication interruptions.

Noting that DGs usually lack stable output power, the present study aimed to design a controller for voltage and frequency control of the islanded microgrid by considering disturbance in the input power of DGs. Based on the literature review, it is evident that no study on voltage and frequency control of microgrids has ever considered the full dynamic model of the resources and microgrid, as well as power disturbances simultaneously. Many references have presented voltage and frequency control but neglected the dynamics of DGs or power input disturbances. Also, some previous studies have discussed input disturbances and the dynamics of DGs, but the only control challenge they have considered has been the frequency control of the microgrid. Indeed, none of the references has been completely modeled.

This paper considers the dynamics of each DG to eliminate power input disturbances, maintain the voltage and frequency within the permissible range, and consequently preserve the microgrid's stability (with electronic power converters). The controller also makes the necessary changes in power electronic settings to eliminate disturbances and accomplish the control objectives.

Accordingly, the highlights of this paper are as follows:

- Presentation of a method for voltage and frequency control of islanded microgrids
- Designing a multi-output controller
- Considering the dynamics of each DG with power converters and power generation uncertainties
- Changing and controlling the switching method of power converters of DGs
- Increasing the velocity of response to changes and maintaining the closed-loop stability.

The rest of the paper is organized as follows. Section 2 discusses multivariable systems and how to design controllers for these systems. In Section 3, the target microgrid is modeled, and mathematical equations are obtained. Section 4 studies the dynamic model of each DG and presents its mathematical equations. Section 5 provides the state-space model of the system and the system matrices for simulation. In Section 6, a simulation is performed according to the equations expressed in Section 5, and the results are presented. Section 7 concludes the paper.

## 2. DESIGNING MULTIVARIABLE CONTROLLERS

### 2.1. Multivariable Linear Systems

Most control system analysis and design systems are based on the system's mathematical model. A system model may be a mathematical and analytical model of the system. Physical

systems and many non-physical systems can be described by a system of nonlinear differential equations and algebraic equations [25, 26]. By linearizing these equations around operating points, we can obtain the system's differential and algebraic linear equations. This way, linear control systems are analyzed and designed around the designated operating points. In the study on multivariable control systems, the system is described by linear state-space models, transfer function matrix, system matrix, and fractional matrix. The description of the space state or internal description is given in (1) and (2) [27]:

$$\dot{x}(t) = A.x(t) + B.u(t) + E.w(t) \quad (1)$$

$$y(t) = C.x(t) + D.u(t) + F.w(t) \quad (2)$$

where vector  $x$  shows the state variables,  $u$  is the input vector,  $y$  is the output vector,  $w$  is the disturbance vector, and the matrices  $A$ ,  $B$ ,  $C$ ,  $D$ ,  $E$ , and  $F$  are dimensioned. The control systems are designed with two objectives: stabilizing and improving the closed-loop operation. If the open-loop system is stable, the main purpose during designing the control system will be to improve the performance of the set of system behaviors. If the exact model of the open-loop system is available, or in other terms, the system's behavior is not uncertain, the desired control objectives can be achieved without feedback. However, practical systems are always associated with some uncertainty, which needs the use of feedback.

## 2.2. Design of a PI Controller for Multivariable Systems

Consider a multivariable system described using the state-space equations and the output shown in Fig. 1.

The corresponding transfer function matrix for the system is obtained as (3) [27]:

$$G(s) = C.(sI - A)^{-1}B \quad (3)$$

where  $G(S)$  is an  $(m \times 1)$  transfer function matrix.

Note that the open-loop system must be stable and controllable for controller design. Therefore, all the eigenvalues of matrix  $A$  should be placed on the left half of the imaginary, which will be proven as follows.

Consider the multivariable system given in (1) and (2). Assuming that the assumptions are correct, the multivariable PI controller is considered as (4):

$$u(s) = (K_1 + \frac{K_2}{s}).e(s) \quad (4)$$

The matrices  $K_1$  and  $K_2$  are defined as:

$$K_1 = \alpha \varepsilon K \quad (5)$$

$$K_2 = \varepsilon K \quad (6)$$

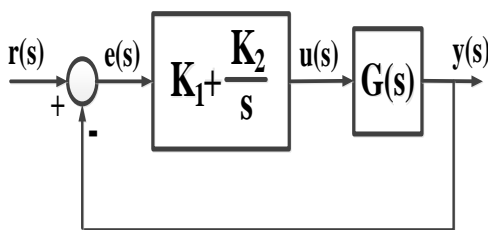


Fig. 1: A multivariable closed-loop system.

where  $\varepsilon$  is a setting parameter,  $\alpha$  is a positive real number, and  $K$  as the design matrix is defined by (7):

$$K = G^T (GG^T)^{-1} \Sigma \quad (7)$$

Here  $G = G(0)$  and  $\Sigma$  is:

$$\Sigma = \begin{bmatrix} \sigma_1 & 0 & \dots & 0 \\ 0 & \sigma_2 & \ddots & \vdots \\ \vdots & \ddots & \ddots & 0 \\ 0 & \dots & 0 & \sigma_m \end{bmatrix} \quad (8)$$

with  $\sigma_i > 0$ .

The most important advantage of the controller designed in this article is the control of multiple parameters, the stability of the closed loop system, and the appropriate response speed. The controller is designed below based on the system matrix.

## 3. MODELING AND MATHEMATICAL EQUATIONS OF THE MICROGRID

The islanded microgrid under study is shown in Fig. 2 [28]. This microgrid involves the interconnection of two DGs via a line and two local complex interconnected loads. This study modeled energy sources using a boost converter and an inverter to the main microgrid with constant loads. Different current (power) oscillations of DG1 are modeled as a disturbance that causes frequency and voltage deviations.

Current equations are written according to the matrix given in (9) [29]:

$$\begin{bmatrix} \vec{I}_1 \\ \vec{I}_2 \end{bmatrix} = \begin{bmatrix} Y_a + Y_c & -Y_c \\ -Y_c & Y_b + Y_c \end{bmatrix} \begin{bmatrix} \vec{V}_{r1} \\ \vec{V}_{r2} \end{bmatrix} \quad (9)$$

According to (9), equation (10) is obtained:

$$\vec{V}_r = Y^{-1} \vec{I} \quad (10)$$

If voltage and current equations are considered in the following sequence, equations (11) and (12) are obtained:

$$\vec{V}_r = V_{r1} + jV_{r2} \quad (11)$$

$$\vec{I} = I_d + jI_q \quad (12)$$

Equations (9) and (10) yield (13), (14), and (15):

$$Z_{11} = \frac{Z_a Z_c + Z_a Z_b}{Z_a + Z_b + Z_c} \quad (13)$$

$$Z_{12} = Z_{21} = \frac{Z_a Z_b}{Z_a + Z_b + Z_c} \quad (14)$$

$$Z_{22} = \frac{Z_a Z_b + Z_b Z_c}{Z_a + Z_b + Z_c} \quad (15)$$

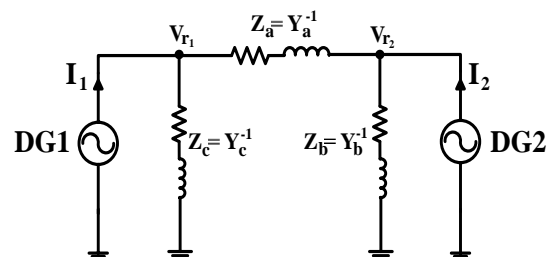


Fig. 2: The studied islanded microgrid [28].

These are also expressed as (16)-(19):

$$Z_{11} = R_{11} + jX_{11} \quad (16)$$

$$Z_{12} = R_{12} + jX_{12} \quad (17)$$

$$Z_{21} = R_{21} + jX_{21} \quad (18)$$

$$Z_{22} = R_{22} + jX_{22} \quad (19)$$

As a result, according to the above equations, equations (20)-(23) are obtained:

$$V_{d1} = R_{11}I_{1d} - X_{11}I_{1q} + R_{12}I_{2d} - X_{12}I_{2q} \quad (20)$$

$$V_{q1} = X_{11}I_{1d} + R_{11}I_{1q} + X_{12}I_{2d} + R_{12}I_{2q} \quad (21)$$

$$V_{d2} = R_{21}I_{1d} - X_{21}I_{1q} + R_{22}I_{2d} - X_{22}I_{2q} \quad (22)$$

$$V_{q2} = X_{21}I_{1d} + R_{21}I_{1q} + X_{22}I_{2d} + R_{22}I_{2q} \quad (23)$$

#### 4. MODELING AND MATHEMATICAL EQUATIONS OF DG UNITS

Both DGs contain a DC/DC converter, an AC/DC inverter, and an LC filter, as shown in Fig. 3. The active power is controlled by the controller's switching function. DC-bus voltage is regulated by the switching function in the dq axis of the inverter. Therefore, the voltage and frequency of buses connected to resources are system outputs, and switching functions are controlled by converters and inverters of each DG. The input disturbance is also considered a change in the input current and, as a result, a change in the generating power of the first DG. The input voltage to the DC/DC converter is determined by the switching function ( $\alpha_i$ ) of each resource. DC-bus voltage ( $V_{DC}$ ) and output current of the converter ( $I_{scr}$ ) are indicated by the switch function ( $\alpha_i$ ) and DG current. The output voltage of each inverter ( $V_{d_i}$  and  $V_{q_i}$ ) is expressed by the switching function ( $K_{d_i}$  and  $K_{q_i}$ ) and the DC-bus voltage ( $V_{DC}$ ). The input current of the inverter ( $I_m$ ) is a function of the switching function ( $K_{d_i}$  and  $K_{q_i}$ ) and the output current ( $I_{d_i}$  and  $I_{q_i}$ ) of the AC bus. The input voltage sources are connected to a DC/DC converter by a resistor and inductor ( $R_{x_i}$  and  $L_{x_i}$ ), as in Fig. 3. The input voltage to the converter ( $V_{h_i}$ ) is a function of the input voltage ( $V_{in_i}$ ), input current ( $I_{in_i}$ ), and resistor and inductor ( $R_{x_i}$  and  $L_{x_i}$ ). The DC/DC converter is filtered by a capacitor ( $C_{dc}$ ) and connected to an AC/DC inverter. The input current to the inverter is equal to the difference between the output current of the converter ( $I_{scr}$ ) and the capacitor current. The inverter output and AC side are modeled in this section. The inverter is connected to the grid by an RL filter, as shown in Fig. 3. The inverter output currents ( $I_{d_i}$  and  $I_{q_i}$ ) are equivalent to the output currents  $I_1$  or  $I_2$ , as given in Fig. 2. In the equations,  $R_{ac_i}$  and  $L_{ac_i}$  are the resistance and inductance of the line,  $V_{d_i}$

and  $V_{q_i}$  are voltages of the bus system in the dq axes, and  $V_{DC}$  is the DC-bus voltage.

In Fig. 3, the input source with an index  $i = 1, 2$  is related to DG1 and DG2, respectively.

The power equation for each of the sources is obtained by (24):

$$P_i = V_{d_i} I_{d_i} + V_{q_i} I_{q_i} \quad (24)$$

Also, equations (25)-(29) are obtained considering the DC/DC converter and the AC/DC inverter:

$$V_{d_i} = K_{d_i} V_{DC_i} \quad (25)$$

$$V_{q_i} = K_{q_i} V_{DC_i} \quad (26)$$

$$I_{scr_i} = \alpha_i I_{in_i} \quad (27)$$

$$V_{h_i} = \alpha_i V_{DC_i} \quad (28)$$

$$I_{m_i} = K_{d_i} I_{d_i} + K_{q_i} I_{q_i} \quad (29)$$

By establishing KVL at the output of each inverter, equations (30) and (31) are expressed:

$$\dot{I}_{d_i} = \frac{-R_{ac_i}}{L_{ac_i}} I_{d_i} + \frac{1}{L_{ac_i}} V_{DC_i} K_{d_i} + \omega_i I_{q_i} - \frac{1}{L_{ac_i}} V_{rd_i} \quad (30)$$

$$\dot{I}_{q_i} = \frac{-R_{ac_i}}{L_{ac_i}} I_{q_i} + \frac{1}{L_{ac_i}} V_{DC_i} K_{q_i} + \omega_i I_{d_i} - \frac{1}{L_{ac_i}} V_{rq_i} \quad (31)$$

On the other hand, according to (27) and (28) and writing a KVL at the input of each converter, Equation (32) is provided:

$$\dot{I}_{in_i} = \frac{1}{L_{x_i}} V_{in_i} - \frac{1}{L_{x_i}} V_{DC_i} \alpha_i - \frac{R_{x_i}}{L_{x_i}} I_{in_i} \quad (32)$$

Also, by writing the KCL in the node to which the capacitor is connected and considering (28) and (29), we have:

$$\dot{V}_{DC_i} = \frac{1}{C_{DC_i}} \alpha_i I_{in_i} - \frac{1}{C_{DC_i}} (K_{d_i} I_{d_i} + K_{q_i} I_{q_i}) \quad (33)$$

The output frequency of each inverter is obtained using the droop character [28]:

$$\omega_i = \omega_{0_i} - K_{p_i} (P - P_{0_i}) \quad (34)$$

To ensure each inverter's voltage and frequency control, their output voltage and frequency are required.

These quantities are measured using a low-pass filter with a cut-off frequency of  $\omega_f$ . According to Fig. 4, the power equation in the Laplace domain is formulated as [28]:

$$P_{meas}(s) = \frac{\omega_f}{s + \omega_f} P(s) \quad (35)$$

By substituting (35) in (34), we have:

$$\dot{\Delta\omega_i} = -\omega_{f_i} \Delta\omega_i - \omega_{f_i} K_{p_i} \Delta P_i \quad (36)$$

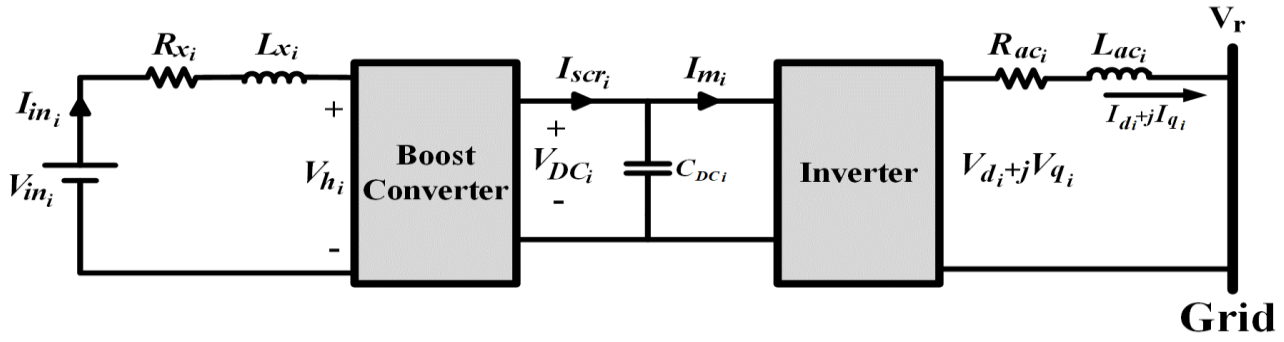


Fig. 3: The dynamics of each DG.

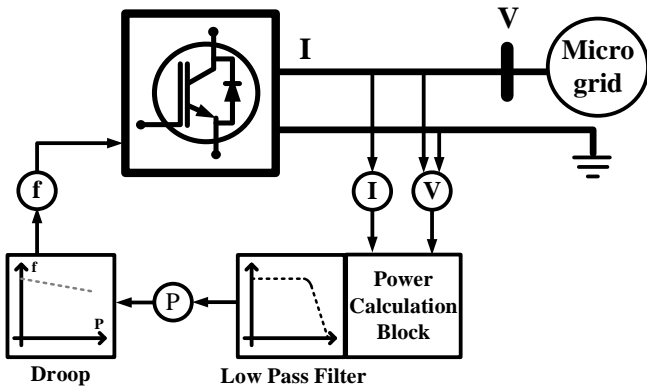


Fig. 4: Diagram of frequency control of each DG unit.

As is seen, these equations are nonlinear, but they should be linear and controllable in the form of state space equations to control the network. The following is allocated to this process.

Fig. 5 shows the performance flowchart of the proposed method.

### 5. STATE-SPACE MODEL OF THE SYSTEM

The state variables ( $\Delta x$ ) include small variations in the DG's input current ( $\Delta I_{in}$ ), DC-bus voltage ( $\Delta V_{DC}$ ), inverter current in the d-axis direction ( $\Delta I_d$ ), inverter current in the q-axis direction ( $\Delta I_q$ ), and output frequency ( $\Delta \omega$ ). Changes, also considered in the output ( $\Delta y$ ), are the variation rate of each parameter from its steady state. Therefore, equations (30)-(33) are linearized around their initial stable points, so we have (37)-(40).

$$\Delta \dot{I}_d = \frac{-R_{ac_i}}{L_{ac_i}} \cdot \Delta I_d + \frac{1}{L_{ac_i}} \cdot V_{DC0_i} \cdot \Delta K_{d_i} + \frac{1}{L_{ac_i}} \cdot K_{d0_i} \cdot \Delta V_{DC_i} + \omega_{0_i} \cdot \Delta I_{q_i} + I_{q0_i} \cdot \Delta \omega_i - \frac{1}{L_{ac_i}} \cdot \Delta V_{rd_i} \quad (37)$$

$$\Delta \dot{I}_q = \frac{-R_{ac_i}}{L_{ac_i}} \cdot \Delta I_q + \frac{1}{L_{ac_i}} \cdot V_{DC0_i} \cdot \Delta K_{q_i} + \frac{1}{L_{ac_i}} \cdot K_{q0_i} \cdot \Delta V_{DC_i} + \omega_{0_i} \cdot \Delta I_{d_i} + I_{d0_i} \cdot \Delta \omega_i - \frac{1}{L_{ac_i}} \cdot \Delta V_{rq_i} \quad (38)$$

$$\Delta \dot{I}_{m_i} = \frac{1}{L_{x_i}} \cdot \Delta V_{in_i} - \frac{1}{L_{x_i}} \cdot \alpha_{0_i} \cdot \Delta V_{DC_i} - \frac{1}{L_{x_i}} \cdot V_{DC0_i} \cdot \Delta \alpha_i - \frac{R_{x_i}}{L_{x_i}} \cdot \Delta I_{m_i} \quad (39)$$

$$\Delta \dot{V}_{DC_i} = \frac{1}{C_{DC_i}} \cdot \alpha_{0_i} \cdot \Delta I_{in_i} + \frac{1}{C_{DC_i}} \cdot I_{in0_i} \cdot \Delta \alpha_i - \frac{1}{C_{DC_i}} (K_{d0_i} \cdot \Delta I_{d_i} + I_{d0_i} \cdot \Delta K_{d_i} + K_{q0_i} \cdot \Delta I_{q_i} + I_{q0_i} \cdot \Delta K_{q0_i}) \quad (40)$$

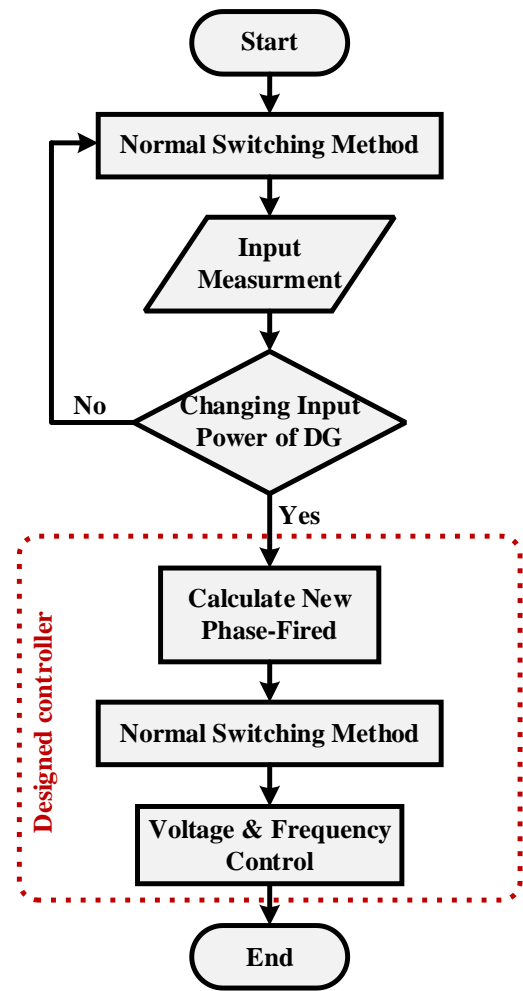


Fig. 5: The performance flowchart of the proposed method.

$\Delta V_{d_i}$  and  $\Delta V_{q_i}$  in (37) and (38) are replaced by the network power flow equation given in (20)-(23). Also, after placing (25)-(26) in (24) and linearizing it,  $\Delta P_i$  is obtained as (36), (see (41)).

In matrices A and B, values with zero indexes are initial values of parameters determined by the dynamics of DG sources and microgrid values, as listed below. In the case of matrices C and W, due to the small variations of voltage across the q-axis, the control of voltage in the q-axis direction is not considered in the literature, and only the control of voltage along the d-axis and the frequency control of each bus are the control objectives. Yet, voltage variations in the q-axis direction are considered in this study. Therefore, the purpose

is to control the frequency and voltage of buses in the d-axis. Therefore, the output matrix C is obtained as (46). Also, in the case of the matrix W, which is the disturbance matrix of the system, this disturbance is only related to the first DG. For the input disturbance to the system, only the change in the input current of the first DG is considered, and in this way, the disturbance matrix (W) is obtained as (47).

Considering the general form of state equations and concerning the linear equations observed in (36)-(41), (42), and (43) are formulated (see (42) and (43)).

Given matrices, matrices A and B are obtained as (44) and (45). Also, according to the dynamical equations of the system, the values of matrices D and F are zero.

$$\Delta \dot{\omega}_i = -\omega_{f_i} \cdot \Delta \omega_i - \omega_{f_i} \cdot K_{P_i} \cdot (I_{d0_i} \cdot (V_{DC0_i} \cdot \Delta K_{d_i} + K_{d0_i} \cdot \Delta V_{DC_i}) + V_{d0_i} \cdot \Delta I_{d_i} + I_{q0_i} \cdot (V_{DC0_i} \cdot \Delta K_{q_i} + K_{q0_i} \cdot \Delta V_{DC_i}) + V_{q0_i} \cdot \Delta I_{q_i}) \quad (41)$$

$$\Delta x = [\Delta I_{d1} \quad \Delta I_{q1} \quad \Delta I_{in1} \quad \Delta V_{DC1} \quad \Delta \omega_1 \quad \Delta I_{d2} \quad \Delta I_{q2} \quad \Delta I_{in2} \quad \Delta V_{DC2} \quad \Delta \omega_2]^T \quad (42)$$

$$\Delta u = [\Delta \alpha_1 \quad \Delta K_{d1} \quad \Delta K_{q1} \quad \Delta \alpha_2 \quad \Delta K_{d2} \quad \Delta K_{q2}]^T \quad (43)$$

$$A = \begin{bmatrix} \frac{-R_{ac1}}{L_{ac1}} - \frac{R_{11}}{L_{ac1}} & \omega_{01} - \frac{X_{11}}{L_{ac1}} & 0 & \frac{K_{d01}}{L_{ac1}} & I_{q01} & -\frac{R_{12}}{L_{ac1}} & \frac{X_{12}}{L_{ac1}} & 0 & 0 & 0 \\ \omega_{01} - \frac{X_{11}}{L_{ac1}} & \frac{-R_{ac1}}{L_{ac1}} - \frac{R_{11}}{L_{ac1}} & 0 & \frac{K_{q01}}{L_{ac1}} & I_{d01} & -\frac{X_{12}}{L_{ac1}} & -\frac{R_{12}}{L_{ac1}} & 0 & 0 & 0 \\ 0 & 0 & -\frac{R_{x1}}{L_{x1}} & -\frac{\alpha_{01}}{L_{x1}} & 0 & 0 & 0 & 0 & 0 & 0 \\ \frac{-K_{d01}}{C_{DC1}} & \frac{-K_{q01}}{C_{DC1}} & \frac{\alpha_{01}}{C_{DC1}} & 0 & 0 & 0 & 0 & 0 & 0 & 0 \\ -\omega_{f1} \cdot K_{P1} \cdot V_{d01} & -\omega_{f1} \cdot K_{P1} \cdot V_{q01} & 0 & -\omega_{f1} \cdot K_{P1} \cdot (I_{d01} \cdot K_{d01} + I_{q01} \cdot K_{q01}) & -\omega_{f1} & 0 & 0 & 0 & 0 & 0 \\ -\frac{R_{21}}{L_{ac2}} & \frac{X_{21}}{L_{ac2}} & 0 & 0 & 0 & \frac{-R_{ac2}}{L_{ac2}} - \frac{R_{22}}{L_{ac2}} & \omega_{02} - \frac{X_{22}}{L_{ac2}} & 0 & \frac{K_{d02}}{L_{ac2}} & I_{q02} \\ -\frac{X_{21}}{L_{ac2}} & -\frac{R_{21}}{L_{ac2}} & 0 & 0 & 0 & \omega_{02} - \frac{X_{22}}{L_{ac2}} & \frac{-R_{ac2}}{L_{ac2}} - \frac{R_{22}}{L_{ac2}} & 0 & \frac{K_{q02}}{L_{ac2}} & I_{d02} \\ 0 & 0 & 0 & 0 & 0 & 0 & 0 & -\frac{R_{x2}}{L_{x2}} & -\frac{\alpha_{02}}{L_{x2}} & 0 \\ 0 & 0 & 0 & 0 & 0 & \frac{-K_{d02}}{C_{DC2}} & \frac{-K_{q02}}{C_{DC2}} & \frac{\alpha_{02}}{C_{DC2}} & 0 & 0 \\ 0 & 0 & 0 & 0 & 0 & -\omega_{f2} \cdot K_{P2} \cdot V_{d02} & -\omega_{f2} \cdot K_{P2} \cdot V_{q02} & 0 & -\omega_{f2} \cdot K_{P2} \cdot (I_{d02} \cdot K_{d02} + I_{q02} \cdot K_{q02}) & -\omega_{f2} \end{bmatrix} \quad (44)$$

$$B = \begin{bmatrix} 0 & \frac{V_{DC01}}{L_{ac1}} & 0 & 0 & 0 & 0 & 0 & 0 & 0 & 0 \\ 0 & 0 & \frac{V_{DC01}}{L_{ac1}} & 0 & 0 & 0 & 0 & 0 & 0 & 0 \\ \frac{-V_{DC01}}{L_{x1}} & 0 & 0 & 0 & 0 & 0 & 0 & 0 & 0 & 0 \\ \frac{I_{in01}}{C_{DC1}} & \frac{-I_{d01}}{C_{DC1}} & \frac{-I_{q01}}{C_{DC1}} & 0 & 0 & 0 & 0 & 0 & 0 & 0 \\ 0 & -\omega_{f1} \cdot K_{P1} \cdot I_{d01} \cdot V_{DC01} & -\omega_{f1} \cdot K_{P1} \cdot I_{q01} \cdot V_{DC01} & 0 & 0 & 0 & 0 & 0 & 0 & 0 \\ 0 & 0 & 0 & 0 & 0 & \frac{V_{DC02}}{L_{ac2}} & 0 & 0 & 0 & 0 \\ 0 & 0 & 0 & 0 & 0 & 0 & 0 & \frac{V_{DC02}}{L_{ac2}} & 0 & 0 \\ 0 & 0 & 0 & 0 & \frac{-V_{DC03}}{L_{x2}} & 0 & 0 & 0 & 0 & 0 \\ 0 & 0 & 0 & 0 & \frac{I_{in02}}{C_{DC2}} & \frac{-I_{d02}}{C_{DC2}} & \frac{-I_{q02}}{C_{DC2}} & 0 & 0 & 0 \\ 0 & 0 & 0 & 0 & 0 & -\omega_{f2} \cdot K_{P2} \cdot I_{d02} \cdot V_{DC02} & -\omega_{f2} \cdot K_{P2} \cdot I_{q02} \cdot V_{DC02} & 0 & 0 & 0 \end{bmatrix} \quad (45)$$

$$C = \begin{bmatrix} 0 & 0 & 0 & 0 & 1 & 0 & 0 & 0 & 0 & 0 \\ R_{11} & -X_{11} & 0 & 0 & 0 & R_{12} & -X_{12} & 0 & 0 & 0 \\ X_{11} & R_{11} & 0 & 0 & 0 & X_{12} & R_{12} & 0 & 0 & 0 \\ 0 & 0 & 0 & 0 & 0 & 0 & 0 & 0 & 0 & 1 \\ R_{21} & -X_{21} & 0 & 0 & 0 & R_{22} & -X_{22} & 0 & 0 & 0 \\ X_{21} & R_{21} & 0 & 0 & 0 & X_{22} & R_{22} & 0 & 0 & 0 \end{bmatrix} \quad (46)$$

$$W = \begin{bmatrix} 0 & 0 & -\frac{R_{x1}}{L_{x1}} & \frac{\alpha_{01}}{C_{DC1}} & 0 & 0 & 0 & 0 & 0 & 0 \end{bmatrix}^T \quad (47)$$

In matrices A and B, values with zero indexes are initial values of parameters determined by the dynamics of DG sources and microgrid values, which are listed below.

In the case of matrices C and W, due to the small variation of voltage across the q-axis, the control of voltage in the q-axis direction is not considered in the literature, and only the control of voltage along the d-axis and the frequency control of each bus are the control objectives. Yet, the voltage changes in the q-axis direction are considered in this study. Therefore, the purpose is to control the frequency and voltage of buses in the d-axis. Thus, the output matrix C is obtained as (46). Also, in the case of matrix W, which is the disturbance matrix of the system, this disturbance is only related to the first DG. For the input disturbance to the system, only the change in the input current of the first DG is considered, and in this way, the disturbance matrix (W) is obtained as (47).

Given that the matrices A, B, C, and W are known and considering the values of the system as listed in Tables 1 and 2, and also assuming that the disturbance to the input current of the first generator is 0.15 A, i.e., almost 1.6% of its steady-state value, the simulations are performed.

Based on Tables 1 and 2, the system's controllability must be examined. According to Section 2.B, for controller design, all eigenvalues of matrix A must have a negative real part. In Table 3, the eigenvalues of matrix A are given.

**Table 1:** The values of the microgrid parameters.

Parameter	Value
$Z_a$	13+6i
$Z_b$	25+13i
$Z_c$	0.5+3i

**Table 2:** The values of DG parameters.

Parameter	Unit	Value for DG1	Value for DG2
$R_{ac}$	$\Omega$	0.5	0.6
$L_{ac}$	mH	5	6
$V_{DC0}$	V	135	140
$I_{d0}$	A	6.4	5.9
$I_{q0}$	A	-3	-2.7
$V_{d0}$	V	127	129.9
$V_{q0}$	V	0	4.7
$f_0$	Hz	50	50
$\omega_0$	rad/sec	100 $\pi$	100 $\pi$
$\omega_f$	rad/sec	37.7	37.7
$C_{CD}$	$\mu$ F	5	4
$K_p$	Hz/watt	0.005	0.006
$R_x$	$\Omega$	0.05	0.05
$L_x$	H	0.03	0.03
$I_{in0}$	A	9	9
$V_{in0}$	V	50	56

**Table 3:** The eigenvalues of matrix A.

The Eigenvalues of Matrix A
100.2 + 6457.80i
-100.2 - 6457.80i
-1682.1 + 6381.9i
-1682.1 - 6381.9i
-3002.8
-0.5
-123.6
-105.6
-36.9
-37.7

## 6. SIMULATION

It is observed that all eigenvalues of matrix A have a negative real part, so the system is stable and has the necessary conditions for controller design. For the system's stability and considering the values of the system matrices (A, B, C, and W), we can design a suitable controller for this system. According to Section 2.B, the controller is implemented using (4)-(8) and applied to the system.

A set of simulation studies is carried out in MATLAB to verify the performance of the proposed controller.

1) Case 1: Given that the disturbance on the first DG's input current is 0.2 A, which is approximately 2.2% of the steady-state value, simulation is performed. Initially, this disturbance was entered as an incremental step in 0.5 seconds.

It is seen that the maximum variation rate is 0.005% for the first bus and 0.007% for the second bus. Also, the maximum voltage variation of each bus in the worst case is 0.59% for the first bus and 0.53% for the second bus, which means the controller can control the voltage and frequency values within the permissible range. If the controller is not used, the change in the frequency of each bus is 10 times, and the voltage change is 5 times as great as that of the case the controller is used. Thus, the controller eliminated the disturbances caused by the variation in input power of the DG and improved the transient and steady-state stability, as illustrated in Figs. 6-8.

2) Case 2: In the next step, the disturbance is applied to the system as a ramp function in 5 seconds. After 3 seconds, the amount of disturbance on the input current of the first DG reaches 0.2 A.

In this case, it is also observed that the controller, while maintaining the transient and steady-state stability, like in case 1, has managed to hold the maximum overshoot of the microgrid frequency in 0.004% and maintain the settling time at time 8 s where the overshoot and settling time decreased 10% and 2 seconds compared to uncontrolled mode. In addition, in this case, frequency changes in buses 1 and 2 are 0.003% and 0.004%, and their voltage changes are 0.02% and 0.025%, respectively, reflecting the proper performance of the designed controller, as shown in Figs. 9-11.

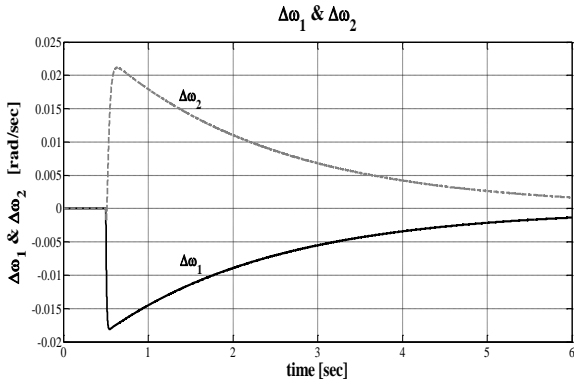


**Fig. 6:** Angle frequency variations for buses 1 and 2 when applying stepping disturbance in the input current of DG1.

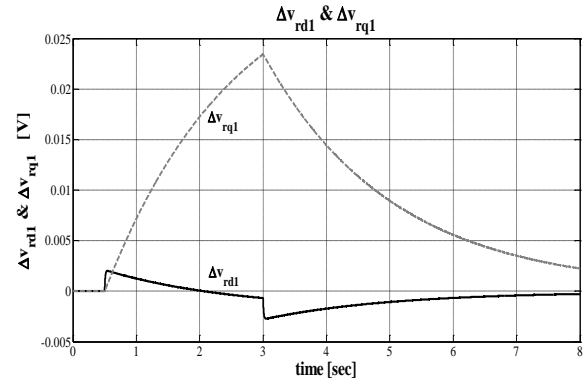


**Fig. 10:** Voltage variation for bus 1 when applying ramping disturbance in the input current of DG1.

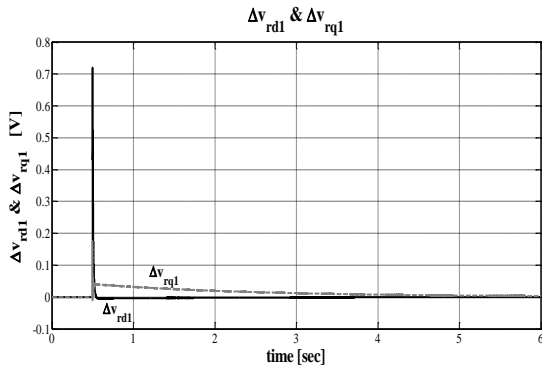


**Fig. 7:** Voltage variation for bus 1 when applying stepping disturbance in the input current of DG1.

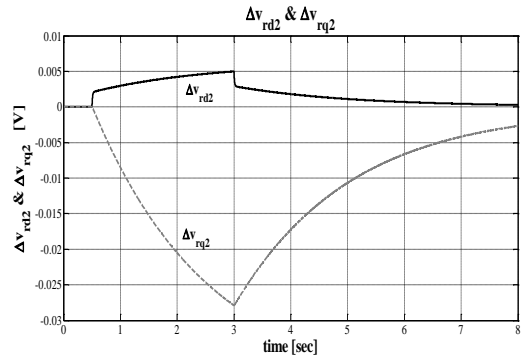


**Fig. 11:** Voltage variation for bus 2 when applying stepping disturbance in the input current of DG1.

### 7. CONCLUSION

In this research, a method was proposed for controlling the voltage and frequency in the islanded microgrid supplied by multiple DGs, considering the uncertainties of the productive power of DGs. Many references have proposed the dynamics of sources by considering the generality of sources. It was observed that the controller can control the frequency and voltage oscillations of each bus caused by the disturbance on the input current of the DG1 and reduce it to zero, where the microgrid supplied the load without any problem. It is worth noting that if the proposed controller is not used, the frequency and voltage of each bus will have a slower response, and higher changes will occur (voltage and frequency have been higher overshoot). Given that the disturbance on the first DG's input current is 0.2 A, which is approximately 2.2% of the steady-state value, simulation was performed, and it was observed that the maximum voltage variation of each bus in the worst case was 0.59% for the first bus and 0.53% for the second bus, which means the controller could control the voltage and frequency values within the permissible range. If the controller is not used, the change in the frequency of each bus will be 10 times and the voltage change will be 5 times as great as that of the case in which the controller is used. In contrast, these changes are greater in other references, so the controller improves frequency and voltage variations. Also, it was observed that the changes in voltage and frequency were dependent on the microgrid parameters and the power change characteristics (amount and duration of change). Voltage and frequency variations depended on the change in power generation and system parameters. In this paper, it was also observed that the controller maintained the closed-loop stability of the system.

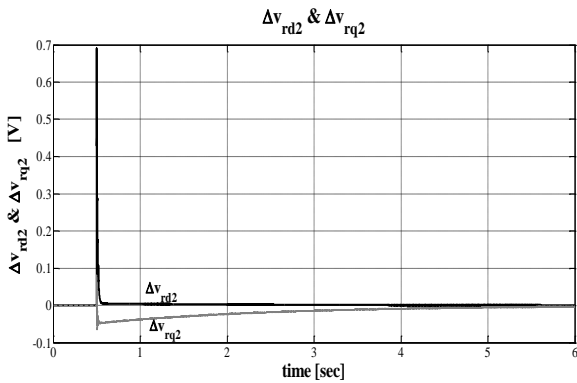


**Fig. 8:** Voltage variation for bus 2 when applying stepping disturbance in the input current of DG1.

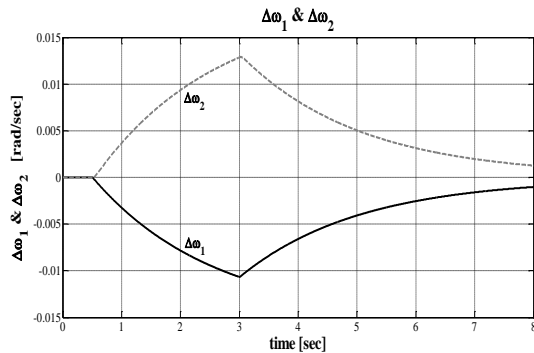


**Fig. 9:** Angle frequency variations for buses 1 and 2 when applying ramping disturbance in the input current of DG1.

In terms of the stability and performance indices against the uncertainties of the input current (input power), it is sufficiently robust and maintains both the bus frequency and voltage in the allowed range. Also, for the controller design, only frequency and output voltage of the inverters are required, so more sensors should be adopted.

#### CREDIT AUTHORSHIP CONTRIBUTION STATEMENT

**Ali Morsagh Dezfuli:** Conceptualization, Data curation, Formal analysis, Methodology, Software, Roles/Writing - original draft, Writing - review & editing. **Mahyar Abasi:** Conceptualization, Methodology, Project administration, Supervision, Validation, Roles/Writing - original draft, Writing - review & editing. **Mohammad Esmail Hasanzadeh:** Conceptualization, Methodology, Validation. **Mahmood Joorabian:** Conceptualization, Methodology, Project administration, Roles/Writing - original draft.

#### DECLARATION OF COMPETING INTEREST

The authors declare that they have no known competing financial interests or personal relationships that could have appeared to influence the work reported in this paper. The ethical issues; including plagiarism, informed consent, misconduct, data fabrication and/or falsification, double publication and/or submission, redundancy has been completely observed by the authors.

#### REFERENCES

- [1] M. Abasi, M. Joorabian, A. Saffarian, and S. G. Seifossadat, "A comprehensive review of various fault location methods for transmission lines compensated by FACTS devices and series capacitors," *Journal of Operation and Automation in Power Engineering*, vol. 9, no.3, pp. 213-225, 2021.
- [2] R. Dhua, S. K. Goswami, and D. Chatterjee, "An optimized frequency and voltage control scheme for distributed generation units of an islanded microgrid," in *Innovations in Energy Management and Renewable Resources*, 2021.
- [3] J. Choi, S.I. Habibi, and A. Bidram, "Distributed finite-time event-triggered frequency and voltage control of AC microgrids," *IEEE Transactions on Power Systems*, vol. 37, no. 3, 2022.
- [4] S. M. Sadeghi, M. Daryalal, and M. Abasi, "Two-stage planning of synchronous distributed generations in distribution network considering protection coordination index and optimal operation situation," *IET Renewable Power Generation*, vol. 16, no. 11, p.p. 2338-2356, 2022.
- [5] A. Saltouh, T. ME, A. El-Shafy A. Nafeh, A. Abou El-Ela, F. H. Fahmy, and Sherif K. Nawar, "Control strategy for seamless transition between grid-connected and islanding modes in microgrid-based PV inverters," *Energy Systems*, vol. 14, no. 4, p.p.1135-1162, 2023.
- [6] M. Yazdani, et al. "Small signal stability of washout filter-based power sharing for an inverter-based microgrid," *The Journal of Engineering*, vol. 2023, no. 2, 2023.
- [7] S. Arunima, and B. Subudhi, "Distributed control for accurate voltage/frequency regulation and power sharing in a microgrid," in *5th International Conference on Energy, Power and Environment: Towards Flexible Green Energy Technologies (ICEPE)*. IEEE, 2023.
- [8] K. Mohammadi, et al, "Asynchronous periodic distributed event-triggered voltage and frequency control of microgrids," *IEEE Transactions on Power Systems*. vol. 36, no. 5, p.p. 4524-4538, 2021.
- [9] Lin, Shin-Wen, and Chia-Chi Chu, "Distributed optimal consensus-based secondary frequency and voltage control of isolated AC microgrids," in *2nd International Conference on Smart Technologies for Power, Energy and Control (STPEC)*, 2021.
- [10] Ning, Boda, Qing-Long Han, and Lei Ding, "Distributed finite-time secondary frequency and voltage control for islanded microgrids with communication delays and switching topologies," *IEEE Transactions on Cybernetics*, vol. 51, no. 8, p.p. 3988-3999, 2020.
- [11] S. Aminzadeh, M. T. Hagh, and H. Seyedi, "Reactive power coordination between solid oxide fuel cell and battery for microgrid frequency control." *Journal of Applied Research in Electrical Engineering*, vol. 1, no. 2, p.p. 121-130, 2022.
- [12] S. Arunima, and B. Subudhi, "Distributed control for accurate voltage/frequency regulation and power sharing in a microgrid," in *5th International Conference on Energy, Power and Environment: Towards Flexible Green Energy, Technologies (ICEPE)*, 2023.
- [13] E. Akbari, "A novel frequency and voltage control method for islanded micro-grid," in *9th Iranian Conference on Renewable Energy & Distributed Generation (ICREDG)*, 2022.
- [14] M. Abasi, M. F. Nezhadnaeini, M. Karimi, N. Yousefi, "A novel meta heuristic approach to solve unit commitment problem in the presence of wind farms," *Revue roumaine des sciences techniques Série Électrotechnique et Énergétique*, vol. 60, no. 3, p.p. 253-262, 2015.
- [15] G. Himanshu, A. Verma, and T. S. Bhatti, "DOBC-based frequency & voltage regulation strategy for PV-diesel hybrid microgrid during islanding conditions," *Renewable Energy*, vol. 196, p.p.883-900, 2022.
- [16] Sh. Hou, J. Chen, and G. Chen, "Distributed control strategy for voltage and frequency restoration and accurate reactive power-sharing for islanded microgrid," *Energy Reports*, vol. 9, p.p. 742-751, 2023.
- [17] M.H. Mousavi, H. M. Cheshmeh Beigi, and M. Ahmadi, "A DDSRF-based VSG control scheme in islanded microgrid under unbalanced load conditions," *Electrical Engineering*, vol. 105, no. 6, p.p. 4321-4337, 2023.
- [18] M. F. Nezhadnaeini, M. Hajivand, M. Abasi, S. Mohajerami, "Optimal allocation of distributed generation units based on different objectives by a novel version group search optimizer algorithm in unbalance load system," *Revue roumaine des sciences techniques*

*Série Électrotechnique et Énergétique*. vol. 61, no. 4, pp. 338–342, 2016.

- [19] M. Dashtdar, et al, "Improving the power quality of island microgrid with voltage and frequency control based on a hybrid genetic algorithm and PSO," *IEEE Access*, vol. 10, p.p. 105352-105365, 2022.
- [20] Sepehrzad, Reza, et al, "Optimal energy management of distributed generation in micro-grid to control the voltage and frequency based on PSO-adaptive virtual impedance method," *Electric Power Systems Research*, vol. 208, 2022.
- [21] Zh. Wu, and H. Cheng, "Fixed-time control of distributed secondary voltage and frequency for microgrids considering state-constrained," *Electrical Engineering*, p.p. 1-13, 2023.
- [22] Grover, Himanshu, Ashu Verma, and T. S. Bhatti, "A fast and robust DOBC based frequency and voltage regulation scheme for future power systems with high renewable penetration." *Energy Conversion and Economics*, vol. 4, no. 4, p.p. 276-291, 2023.
- [23] M. Zhai, et al, "Distributed secondary voltage control of microgrids with actuators bias faults and directed communication topologies: Event-triggered approaches," *International Journal of Robust and Nonlinear Control*, vol. 32, no.7, p.p. 4422-4437, 2022.
- [24] Pham, Xuan Hoa Thi, "Improved power controller for enhancement of voltage quality in microgrid," *The Journal of Engineering*, vol. 2022, no. 8, p.p. 773-787, 2022.
- [25] M. Abasi, A. T. Farsani, A. Rohani, and M. A. Shiran, "Improving differential relay performance during cross-country fault using a fuzzy logic-based control algorithm," in *5th Conference on Knowledge-Based Engineering and Innovation, Iran*, 2019. IEEE Index.
- [26] M. Abasi, A. T. Farsani, A. Rohani, and A. Beigzadeh, "A novel fuzzy theory-based differential protection scheme for transmission lines," *International Journal of Integrated Engineering*, vol. 12, no. 8, pp. 149-160, 2020.
- [27] M. M. Seron, J. H. Braslavsky, and G.C. Goodwin, "MIMO control. In: Fundamental limitations in filtering and control," *Communications and Control Engineering*. Springer, London, 1997.
- [28] E. A. A. Coelho, P. C. Cortizo, and P. F. D. Garcia, "Small-signal stability for parallel-connected inverters in stand-alone AC supply systems," *IEEE Transactions on Industry Applications*, vol.38, Issue.2, 2002.
- [29] M. Abasi, N. Heydarzadeh, and A. Rohani, "Broken conductor fault location in power transmission lines using GMDH function and single-terminal data independent of line parameters," *Journal of Applied Research in Electrical Engineering*, vol. 1, no. 1, 2021.

## BIOGRAPHY



**Ali Morsagh Dezfali** was born in Dezfali, Iran in 1992. He received his B.Sc. degree from the Jundi-Shapur University of Technology of Dezfali, Dezfali, Iran in 2015 and his M.Sc. degree from Shahid Rajaei Teacher Training University, Tehran, Iran in 2017, both in Power Electrical Engineering. He is currently a Ph.D. candidate in Power Electrical Engineering at Shahid Chamran University, Ahvaz, Iran. His research interests are voltage and frequency control of microgrids, power electronics, FACTS devices, and power system protection.



**Mahyar Abasi** was born in 1989 in Iran. He graduated with a Ph.D. in Electrical Power Engineering from Shahid Chamran University, Ahvaz, Iran in 2021. He has more than 60 published journal and conference papers, more than 10 authored books, 11 industrial research projects, and a patent in power systems. In 2021, he was introduced as the top researcher of Khuzestan province, Iran, and in the years 2021 to 2023, he was successful in receiving four titles from the membership schemes of the National Elite Foundation in Iran. He is currently an assistant professor in the Electrical Engineering department of Arak University, Arak, Iran. His specialized interests are fault protection, detection, classification, and location in HVAC and HVDC transmission lines, control of reactive power and FACTS devices, evaluation and improvement of power quality, and power system studies.



power electronics.

**Mohammad Esmail Hassanzadeh** received his MSc. and Ph.D. degrees from the Shiraz University of Technology, Iran, in 2015 and 2022, respectively. He is currently an assistant professor in electrical engineering at Firouzabad Higher Education Center, Shiraz University of Technology. His research interests include power system stability and optimization, microgrids, renewable energies, FACTS devices, and



**Mahmood Joorabian** was born in Iran in 1961. He received his BEE degree from the University of New Haven, CT, USA, M.Sc. degree in Electrical Power Engineering from Rensselaer Polytechnic Institute, NY, USA, and a Ph.D. degree in Electrical Engineering from the University of Bath, Bath, UK in 1983, 1985 and 1996, respectively. He has been with the Department of Electrical Engineering at Shahid Chamran University, Ahvaz, Iran, as a Senior Lecturer (1985), Assistant Professor (1996), Associate Professor (2004), and Professor (2009). His main research interests are fault location, FACTS devices, power system protection, power quality, and applications of intelligence techniques in power systems.

## Copyrights

© 2024 Licensee Shahid Chamran University of Ahvaz, Ahvaz, Iran. This article is an open-access article distributed under the terms and conditions of the Creative Commons Attribution NonCommercial 4.0 International (CC BY-NC 4.0) License (<http://creativecommons.org/licenses/by-nc/4.0/>).

